Natural Energy Decomposition Analysis: Explicit Evaluation of Electrostatic and Polarization Effects with Application to Aqueous Clusters of Alkali Metal Cations and Neutrals

Eric D. Glendening*

Contribution from the Environmental Molecular Sciences Laboratory, Pacific Northwest Laboratory, Richland, Washington 99352

Received June 6, 1995. Revised Manuscript Received December 29, 1995[⊗]

Abstract: Natural energy decomposition analysis (NEDA) is extended to calculate electrostatic and polarization contributions. NEDA is a Hartree−Fock-based approach that facilitates the calculation of the electrostatic, polarization, charge transfer, exchange, and deformation components of intermolecular interactions. Analysis of the aqueous clusters of the alkali metal cations, $M^+(H_2O)_n$ ($n = 1-4$), demonstrates the reasonable behavior of the NEDA components and dipole moments with changes in geometry and coordination. In general, the electrostatic and polarization components behave as anticipated from a classical treatment based on point charges, dipoles, and polarizabilities. Extended basis set applications demonstrate the high numerical stability of the method whereas comparison calculations with the Morokuma analysis show contrastingly poor basis set convergence. The popular 6-31+G* basis set yields a binding energy for $Li^+(H_2O)$ in good agreement with the estimated complete basis set (CBS) limit. However, comparison of the 6-31+G* and CBS NEDA results reveals that this agreement is fortuitous, relying on a cancellation of errors that stem from the inability of this basis set to accurately describe the dipole moment and polarizability of water. Representative calculations are also presented for open-shell clusters $Na(H_2O)_n$ ($n = 1-4$) at the unrestricted-Hartree−Fock level.

I. Introduction

Computational tools for interpreting electronic structure calculations provide valuable insight into the various factors that influence molecular interactions. The partitioning scheme of Morokuma and co-workers[1−3] is perhaps the most popular of numerous methods proposed to analyze interactions at the Hartree−Fock level. This procedure evaluates electrostatic, polarization, charge transfer, and exchange repulsion energies, the essential elements that form the basis for our conceptual models of intermolecular forces.[4]

We recently proposed an alternative approach for analyzing molecular interactions, natural energy decomposition analysis (NEDA).[5] NEDA partitions the interaction energy into electrostatic, charge transfer, and deformation components based on the natural bond orbital (NBO) method of Weinhold and co-workers.[6−8] Applications were demonstrated for interactions of varying strength, from weak hydrogen bonds in the water dimer to stronger ionic bonds in the alkali hydrides and donor−acceptor interactions in BH_3NH_3 and BH_3CO. Analyses of ion−molecule interactions in cation−ether and cation−crown ether clusters have also been reported.[9−12]

NEDA offers several advantages over the Morokuma scheme. Most importantly, the NEDA components exhibit high numerical stability, whereas the Morokuma analysis is fairly sensitive to basis set level. The basis set dependence of the latter stems from the calculation of an intermediate wave function that is not antisymmetric. Variational optimization of this wave function potentially leads to the collapse of the valence electrons of one fragment into the core orbitals of its neighbor, resulting in a fortuitously strong polarization component.[13,14] NEDA also evaluates the electric moments of the individual molecular fragments that comprise the complex. This feature thus provides a quantitative measure of the degree of polarization that the fragments undergo in the field of the adjacent fragments.

The purpose of the present work is threefold. First, we describe an extension of NEDA for explicit calculation of separate electrostatic and polarization contributions. The polarization component was not evaluated separately in the original treatment.[5] Rather, it was included as part of the electrostatic contribution. Second, we demonstrate the method by analyzing the interactions of alkali metal cations with water in the clusters $M^+(H_2O)_n$ ($n = 1-4$). These clusters were chosen as a first application of the modified approach since they exhibit important polarization effects and are well described at the Hartree−Fock level.[11,15,16] Finally, we examine clusters of Na atom with water, $Na(H_2O)_n$ ($n = 1-4$). These representative calculations

* Permanent address: Department of Chemistry, Indiana State University, Terre Haute, IN 47809. Electronic mail: chglen@scifac.indstate.edu.

[⊗] Abstract published in *Advance ACS Abstracts,* March 1, 1996.

(1) Morokuma, K. *J. Chem. Phys.* **1971**, *55*, 1236.
(2) Kitaura, K.; Morokuma, K. *Int. J. Quantum Chem.* **1976**, *10*, 325.
(3) Morokuma, K. *Acc. Chem. Res.* **1977**, *10*, 294.
(4) van Lenthe, J. H.; van Duijneveldt-van de Rijdt, J. G. C. M.; van Duijneveldt, F. B. In *Ab Initio Methods in Quantum Chemistry*; Lawley, K. P., Ed.; Wiley: New York, 1987; Vol. II, p 521.
(5) Glendening, E. D.; Streitwieser, A. *J. Chem. Phys.* **1994**, *100*, 2900.
(6) Foster, J. P.; Weinhold, F. *J. Am. Chem. Soc.* **1980**, *102*, 7211.
(7) Reed, A. E.; Weinstock, R. B.; Weinhold, F. *J. Chem. Phys.* **1985**, *83*, 735.
(8) Reed, A. E.; Curtiss, L. A.; Weinhold, F. *Chem. Rev.* **1988**, *88*, 899.
(9) Glendening, E. D.; Feller, D.; Thompson, M. A. *J. Am. Chem. Soc.* **1994**, *116*, 10657.
(10) Thompson, M. A.; Glendening, E. D.; Feller, D. *J. Phys. Chem.* **1994**, *98*, 10465.
(11) Glendening, E. D.; Feller, D. *J. Phys. Chem.* **1995**, *99*, 3060.
(12) More, M. B.; Glendening, E. D.; Ray, D.; Feller, D.; Armentrout, P. B. *J. Phys. Chem.* Accepted for publication.
(13) Frey, R.; Davidson, E. R. *J. Chem. Phys.* **1989**, *90*, 5555.
(14) Cybulski, S. M.; Scheiner, S. *Chem. Phys. Lett.* **1990**, *166*, 57.
(15) Feller, D.; Glendening, E. D.; Kendall, R. A.; Peterson, K. A. *J. Chem. Phys.* **1994**, *100*, 4981.
(16) Feller, D.; Glendening, E. D.; Woon, D. E.; Feyereisen, M. W. *J. Chem. Phys.* **1995**, *103*, 3526.

0002-7863/96/1518-2473$12.00/0

demonstrate the extension of NEDA for treating open-shell interactions at the unrestricted Hartree−Fock (UHF) level.

II. Natural Energy Decomposition Analysis

We begin by reviewing the NEDA approach and presenting an extension of the original treatment[5] for explicit calculation of electrostatic and polarization contributions. NEDA is based on the NBO analysis of Weinhold and co-workers.[6−8] Given the density matrix, the NBO procedure calculates a set of mutually orthogonal bond orbitals (the NBOs) that, aside from small orthogonalization tails, are strictly localized either on single atoms (core orbitals, lone pairs) or on atom pairs (bonds, antibonds). The molecular fragments of a cluster are naturally defined by the connectivity of the bonds. Thus, for example, the NBO procedure calculates six formally occupied orbitals for $Li^+(H_2O)$, the 1s core, two OH bonds, and two lone pairs that together comprise the water molecule, and the 1s core of Li^+. NEDA employs the Fock matrix expressed in the NBO basis. Hence, we limit our discussion here to the closed-shell, restricted Hartree−Fock (RHF) method. Extension of NEDA to treat open-shell systems at the unrestricted Hartree−Fock level of theory is relatively straightforward. Section VI presents representative open-shell applications.

The binding energy of a complex formed by the association of two fragments is defined as

$$\Delta E = E(\psi_{AB}) - E(\psi_A) - E(\psi_B) \tag{1}$$

where ψ_{AB}, ψ_A, and ψ_B are respectively the variationally optimized wave functions for the AB complex and the isolated fragments A and B. For convenience, we assume all wave functions (including ψ_A and ψ_B) are calculated in the complete AB basis set so that ΔE corresponds to the counterpoise (CP) corrected binding energy of Boys and Bernardi.[17] Furthermore, we constrain the geometries of A and B to remain unchanged during the association reaction so that geometries of fragments within the complex are identical to those at infinite separation. The binding energy therefore contains no contribution from the geometrical distortion of A and B during formation of the complex.

NEDA partitions the CP-corrected binding energy into electrostatic, polarization, charge transfer, exchange, and deformation components,

$$\Delta E = \mathrm{ES} + \mathrm{POL} + \mathrm{CT} + \mathrm{EX} + \mathrm{DEF} \tag{2}$$

This partitioning scheme differs in two respects from that presented in the original paper.[5] First, it includes two contributions (POL and EX) that were not previously considered separately. The ES, POL, and EX terms of eq 2 together comprise the ES component of the original treatment. Second, the original treatment was defined with respect to the uncorrected binding energy so that the partitioning scheme included a basis set superposition error (BSSE) component. This component has been discarded since BSSE is unphysical, an artifact of an incomplete basis set, and because the implementation of NEDA[18] employs the CP correction which approximately treats BSSE.

Evaluating the components of eq 2 relies on the calculation of three intermediate wave functions. Two of these are the fragment wave functions ψ_A^{def} and ψ_B^{def} that are calculated from the eigenvectors of the A and B blocks of the NBO Fock matrix

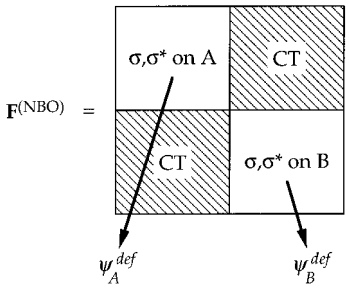

Figure 1. Partitioning of the NBO Fock matrix for the AB complex. The wave functions ψ_A^{def} and ψ_B^{def} are constructed from the eigenvectors of the A, B blocks of this matrix. The off-diagonal blocks describe the CT interactions between A and B that are effectively neglected in the calculation of ψ_{AB}^{loc}.

for the AB complex (cf. Figure 1). For instance, if one of the fragments is a water molecule, the wave function $\psi_{H_2O}^{def}$ is constructed as an antisymmetric product of the five lowest energy eigenvectors (obtained from the appropriate block of the Fock matrix). These eigenvectors correspond to the 1s core, two OH bonds, and two lone pairs of water. Since the NBOs form a set of mutually orthogonal basis functions, ψ_A^{def} and ψ_B^{def} are orthogonal. The third intermediate is the localized wave function ψ_{AB}^{loc} formed from the antisymmetric product of the fragment wave functions,

$$\psi_{AB}^{loc} = A(\psi_A^{def} \cdot \psi_B^{def}) \tag{3}$$

where A is the antisymmetrizer. Note that ψ_{AB}^{loc} is localized in the sense that interfragment electron delocalization (charge transfer) is prevented; ψ_A^{def} and ψ_B^{def} each effectively describe an integer number of electrons. The NEDA components are evaluated using the three intermediate wave functions together with the variationally converged wave functions of eq 1.

Two of the components, CT and DEF, remain unchanged from the original treatment. CT, defined as

$$\mathrm{CT} = E(\psi_{AB}) - E(\psi_{AB}^{loc}) \tag{4}$$

is a stabilizing component that arises from the delocalization of electrons between A and B. DEF has a contribution from each fragment

$$\mathrm{DEF} = \mathrm{DEF(A)} + \mathrm{DEF(B)} \tag{5a}$$

where, for example, the contribution from A is given by

$$\mathrm{DEF(A)} = E(\psi_A^{def}) - E(\psi_A) \tag{5b}$$

Note that this is a positive (repulsive) quantity since ψ_A, the variationally converged wave function for A, is necessarily of lower energy than ψ_A^{def}. For large A−B separations, deformation is primarily the energy cost to polarize the fragment charge distribution in the electric field of the neighboring fragment. For much smaller separations, particularly for fragments within van der Waals' contact, deformation is most closely associated with Pauli repulsions that prevent the charge distribution of one fragment from significantly penetrating that of its neighbor.

We attribute the remaining portion of the binding energy to electrostatic interaction, polarization, and exchange,

$$\mathrm{ES} + \mathrm{POL} + \mathrm{EX} = E(\psi_{AB}^{loc}) - E(\psi_A^{def}) - E(\psi_B^{def}) \tag{6}$$

This contribution was previously assigned to ES alone. The right-hand side of eq 6 can be re-expressed using standard notation[19] in the form

(17) Boys, S. F.; Bernardi, F. *Mol. Phys.* **1970**, *19*, 553.

(18) NBO 4.0: Glendening, E. D.; Badenhoop, J. K.; Reed, A. E.; Carpenter, J. E.; Weinhold, F., Theoretical Chemistry Institute: Madison, WI, 1994.

$$\sum_{\alpha}^{\text{on A}}\sum_{\beta}^{\text{on B}}\frac{Z_\alpha Z_\beta}{R_{\alpha\beta}} - 2\sum_{\alpha}^{\text{on A}}\sum_{b}^{\text{on B}}\left\langle b\left|\frac{Z_\alpha}{R_\alpha}\right|b\right\rangle - 2\sum_{a}^{\text{on A}}\sum_{\beta}^{\text{on B}}\left\langle a\left|\frac{Z_\beta}{R_\beta}\right|a\right\rangle + 4\sum_{a}^{\text{on A}}\sum_{b}^{\text{on B}}(aa|bb) - 2\sum_{a}^{\text{on A}}\sum_{b}^{\text{on B}}(ab|ab) \quad (7)$$

where the orbitals $\{\varphi_a\}$ and $\{\varphi_b\}$ are respectively the doubly occupied eigenvectors of the A and B blocks of the Fock matrix (cf. Figure 1). The first four terms of this expression resemble the classical electrostatic contributions (nuclear−nuclear repulsion, nuclear−electron attraction, and electron−electron repulsion) that are calculated by alternative decomposition schemes, such as the Morokuma analysis.[1−3] However, this interaction involves the distorted charge distributions of ψ_A^{def} and ψ_B^{def} rather than the unperturbed distributions of ψ_A and ψ_B. The last term arises from the exchange interactions of electrons on A with those on B. We now describe the partitioning of eq 7 into ES, POL, and EX components.

The electrostatic interaction component is defined as

$$\text{ES} = \sum_{\alpha}^{\text{on A}}\sum_{\beta}^{\text{on B}}\frac{Z_\alpha Z_\beta}{R_{\alpha\beta}} - 2\sum_{\alpha}^{\text{on A}}\sum_{b'}^{\text{on B}}\left\langle b'\left|\frac{Z_\alpha}{R_\alpha}\right|b'\right\rangle - 2\sum_{a'}^{\text{on A}}\sum_{\beta}^{\text{on B}}\left\langle a'\left|\frac{Z_\beta}{R_\beta}\right|a'\right\rangle + 4\sum_{a'}^{\text{on A}}\sum_{b'}^{\text{on B}}(a'a'|b'b') \quad (8)$$

where the orbitals $\{\varphi_{a'}\}$ and $\{\varphi_{b'}\}$ are the doubly occupied molecular orbitals (MOs) of the infinitely separated fragments. ES is essentially identical to that evaluated by the Morokuma approach except that the MOs of eq 8 are calculated in the full basis set of the AB complex rather than the individual fragment sets. The polarization component is defined as

$$\text{POL} = -2\sum_{\alpha}^{\text{on A}}\sum_{b}^{\text{on B}}\left\langle b\left|\frac{Z_\alpha}{R_\alpha}\right|b\right\rangle - 2\sum_{a}^{\text{on A}}\sum_{\beta}^{\text{on B}}\left\langle a\left|\frac{Z_\beta}{R_\beta}\right|a\right\rangle + 4\sum_{a}^{\text{on A}}\sum_{b}^{\text{on B}}(aa|bb) + 2\sum_{\alpha}^{\text{on A}}\sum_{b'}^{\text{on B}}\left\langle b'\left|\frac{Z_\alpha}{R_\alpha}\right|b'\right\rangle + 2\sum_{a'}^{\text{on A}}\sum_{\beta}^{\text{on B}}\left\langle a'\left|\frac{Z_\beta}{R_\beta}\right|a'\right\rangle - 4\sum_{a'}^{\text{on A}}\sum_{b'}^{\text{on B}}(a'a'|b'b') \quad (9)$$

POL arises from the extra electrostatic interaction associated with the deformation (or polarization) of the unperturbed MOs of the separated fragments to those of the complex ($\{\varphi_{a'}\} \rightarrow \{\varphi_a\}$; $\{\varphi_{b'}\} \rightarrow \{\varphi_b\}$). The exchange component is given by

$$\text{EX} = -2\sum_{a}^{\text{on A}}\sum_{b}^{\text{on B}}(ab|ab) \quad (10)$$

and is an attractive contribution to the binding energy arising from the exchange interactions of electrons on A with those on B.

It is, at times, convenient to use a reference fragment geometry that differs from that of the complex. In these cases, we evaluate a distortion (DIS) component

$$\text{DIS} = \text{DIS(A)} + \text{DIS(B)} \quad (11a)$$

$$\text{DIS(A)} = E(\bar{\psi}_A) - E(\bar{\psi}_A^0) \quad (11b)$$

where $\bar{\psi}_A^0$ is the variationally converged wave function for the fragment A in the chosen reference geometry. The bars indicate that these wave functions are calculated in the fragment basis set only, rather than the full AB basis set used for all other wave function evaluations.

The dipole moment induced on a fragment by the electric field of an adjacent fragment can be calculated using the intermediate wave functions ψ_A^{def} and ψ_B^{def}. For example, the induced moment on A is defined as

$$\Delta\mu_A = \mu(\psi_A^{\text{def}}) - \mu(\psi_A) \quad (12)$$

where $\mu(\psi_A^{\text{def}})$ is the dipole moment of A within the complex and $\mu(\psi_A)$ is the static dipole of the fragment at infinite separation. As demonstrated below, the induced dipoles exhibit behavior similar to that predicted by a classical treatment of polarization in which a polarizable charge distribution interacts with the static moments of its neighbor.

The extensions of the NEDA method described here have been implemented in the GAMESS[20] version of the NBO program.[18] The method can be applied to RHF and UHF wave functions using either the conventional disk-based or direct two-electron integral techniques. Additional details of the implementation were given in the original report.[5] The calculation of the ES, POL, and EX components of eqs 8−10 adds little computational expense, requiring only one additional pass over the one- and two-electron integrals. Unless otherwise indicated, all calculations reported here employed the GAMESS program.[20]

III. Numerical Stability of the NEDA Method

The high numerical stability of the NEDA approach is revealed in the limited basis set dependence of its components. To demonstrate this stability, we examined the $Li^+(H_2O)$ complex using Dunning's correlation consistent basis sets.[21,22] The geometry of the complex was fixed in a C_{2v} configuration with a Li−O distance of 1.85 Å and experimentally determined water geometry [R(OH) = 0.9572 Å, ∠(HOH) = 104.52°].[23] The calculations employed both the standard cc-pVXZ and augmented aug-cc-pVXZ basis sets (X = D, T, and Q) with Cartesian 6-term *d*, 10-term *f*, and 15-term *g* functions rather than the usual spherical components.

Figure 2 shows the calculated binding energy and components of $Li^+(H_2O)$ as a function of basis set level. Two characteristics of the NEDA method are clearly revealed. First, the components are remarkably stable with respect to basis set extension, essentially converged at the triple-ζ level. In fact, the variation of these quantities with increasing basis set level does not differ significantly from that calculated for Δ*E*. ES and POL exhibit slightly greater basis set dependence than Δ*E*, but this is reasonable considering that the standard sets (cc-pVDZ, in particular) tend to overestimate the dipole moment and underestimate the polarizability of the water molecule (*vide infra*).[24] Second, Δ*E* and the NEDA components appear to converge roughly exponentially with increasing basis set level. This behavior has been observed previously for various one- and two-electron properties and can be exploited to estimate complete basis set (CBS) limiting values.[24−31]

(19) Szabo, A.; Ostlund, N. S. *Modern Quantum Chemistry*; McGraw-Hill: New York, 1989.

(20) Schmidt, M. W.; Baldridge, K. K.; Boatz, J. A.; Elbert, S. T.; Gordon, M. S.; Jensen, J. H.; Koseki, S.; Matsunaga, N.; Nguyen, K. A.; Su, S.; Windus, T. L.; Dupuis, M.; Montgomery, J. A., Jr. *J. Comput. Chem.* **1993**, *14*, 1347.

(21) Dunning, T. H., Jr. *J. Chem. Phys.* **1989**, *90*, 1007.

(22) Kendall, R. A.; Dunning, T. H., Jr.; Harrison, R. J. *J. Chem. Phys.* **1992**, *96*, 6796.

(23) Benedict, W. S.; Gailar, N.; Plyler, E. K. *J. Chem. Phys.* **1956**, *24*, 1139.

(24) Feller, D. *J. Chem. Phys.* **1993**, *98*, 7059.

(25) Feller, D. *J. Chem. Phys.* **1992**, *96*, 6104.

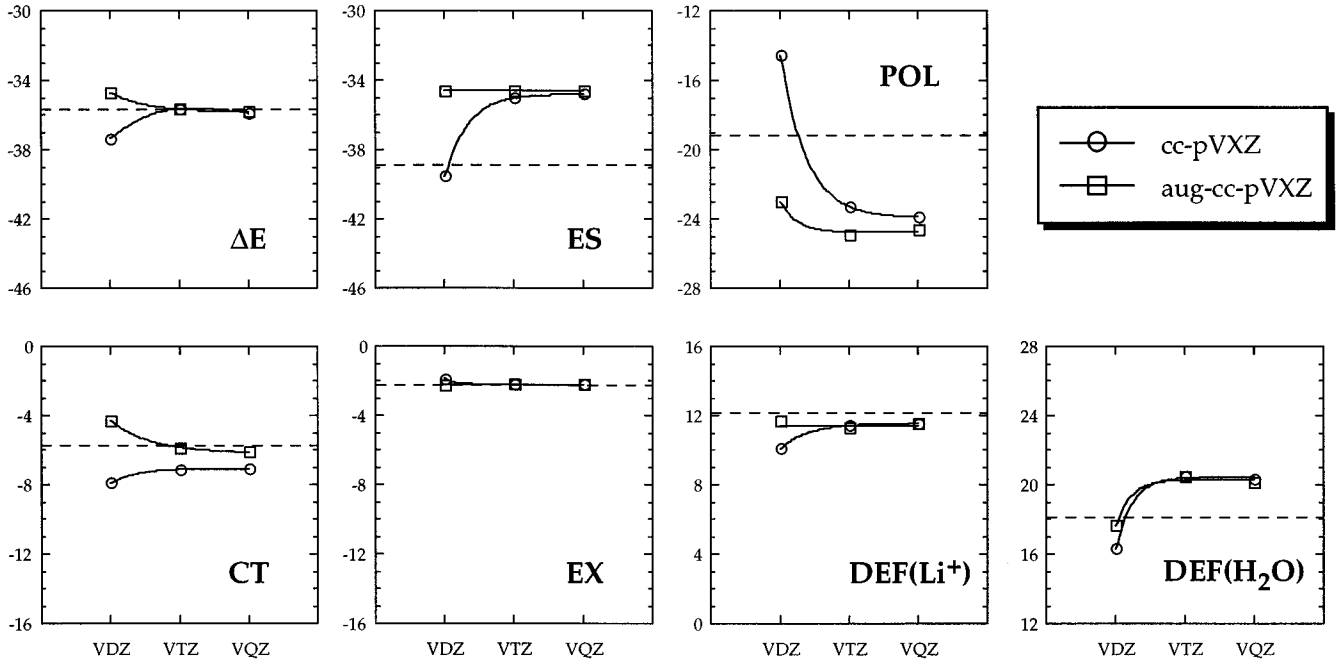

Figure 2. Convergence of the NEDA components (in kcal mol^{-1}) for $Li^+(H_2O)$ as a function of basis set level. The solid curves are obtained from exponential fits (eq 13) of the raw cc-pVXZ and aug-cc-pVXZ values. The dashed lines represent the corresponding values calculated with the 6-31+G* basis set.

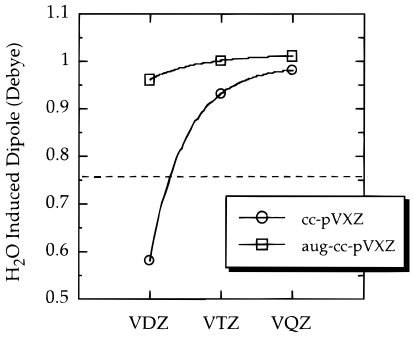

Figure 3. Similar to Figure 1, for the induced dipole moment on the water molecule of $Li^+(H_2O)$.

Estimates of the CBS limits are obtained using a three-parameter, exponential function of the form

$$A(x) = A_{CBS} + A_0 \exp(-\alpha x) \qquad (13)$$

The index x in this expression is the integer 2, 3, or 4 corresponding to the basis set level VDZ, VTZ, or VQZ, respectively. The curves shown in Figure 2 are obtained by fitting eq 13 to the cc-pVXZ and aug-cc-pVXZ data points. The raw data are listed in the supporting information together with estimates of the CBS limits (A_{CBS} of eq 13). Figure 3 shows the induced dipole moment (eq 12) of the water molecule in $Li^+(H_2O)$ as a function of basis set level. The data in this figure were also fit by eq 13 to obtain limiting values for the induced dipole.

The Morokuma analysis[1-3] does not exhibit the high numerical stability of the NEDA approach. For comparison, we performed a parallel series of calculations on the $Li^+(H_2O)$ complex, evaluating the electrostatic interaction (ES), polarization (PL), charge transfer (CT), and exchange (EX) contributions of this alternative method.[1] Calculations were performed with the MELDF programs[32] and the resulting data were fit with eq 13 to estimate the apparent CBS limits for each component. Results are presented in Figure 4. PL and CT are, at best, slowly converging quantities. As argued previously,[13,14] the poor convergence behavior of these components likely stems from the variational optimization of an intermediate wave function that lacks antisymmetry. Kitaura and Morokuma[2] proposed a modification of Morokuma's original method[1] that employed an alternative definition for CT, but the evaluation of PL remained unchanged. Thus, the modified approach should also exhibit poor convergence behavior.

NEDA reveals the electrostatic nature of the Li^+−water interaction. The binding energy (−35.8 kcal mol^{-1} at the aug-cc-pVXZ extrapolated CBS limit) is dominated by ES (−34.6 kcal mol^{-1}), which describes the interaction of the static cation and water charge distributions. ES can be compared to the point charge-dipole approximation,[33,34] $-q\mu/R^2$, where $q = +1$ is the charge representing the cation, $\mu = 1.98$ D is the water dipole moment (the Hartree−Fock limit reported by Feller[24]), and $R = 1.915$ Å is roughly the distance of the cation from the center of mass of the water molecule. This approximation yields a value of −37.3 kcal mol^{-1}, in fair agreement with the ES.

Polarization of the charge distributions further stabilizes $Li^+(H_2O)$. POL is −24.7 kcal mol^{-1}, arising principally from the polarization of the water charge distribution in the field of Li^+. The point charge-dipole approximation,[33,34] $-q\Delta\mu/R^2$, yields a value of −18.8 kcal mol^{-1}, in fair accord with POL.

(26) Woon, D. E.; Dunning, T. H., Jr. *J. Chem. Phys.* **1993**, *99*, 1914.
(27) Peterson, K. A.; Kendall, R. A.; Dunning, T. H., Jr. *J. Chem. Phys.* **1993**, *99*, 1930.
(28) Peterson, K. A.; Kendall, R. A.; Dunning, T. H., Jr. *J. Chem. Phys.* **1993**, *99*, 9790.
(29) Peterson, K. A.; Woon, D. E.; Dunning, T. H., Jr. *J. Chem. Phys.* **1994**, *100*, 7410.
(30) Woon, D. E.; Dunning, T. H., Jr. *J. Chem. Phys.* **1994**, *101*, 8877.
(31) Peterson, K. A.; Dunning, T. H., Jr. *J. Chem. Phys.* **1995**, *102*, 2032.
(32) MELDF: McMurchie, L.; Elbert, S.; Langhoff, S.; Davidson, E. R., The University of Washington, Indiana University, and the Environmental Molecular Sciences Laboratory, 1993. The MELDF suite of programs was substantially modified by D. Feller, R. Cave, D. Rawlings, R. Frey, R. Daasch, L. Nitchie, P. Phillips, K. Iberle, C. Jackels, and E. R. Davidson. The Morokuma analysis was implemented by D. Feller.
(33) Buckingham, A. D. *Adv. Chem. Phys.* **1967**, *12*, 107.
(34) Buckingham, A. D.; Fowler, P. W.; Hutson, J. M. *Chem. Rev.* **1988**, *88*, 963.

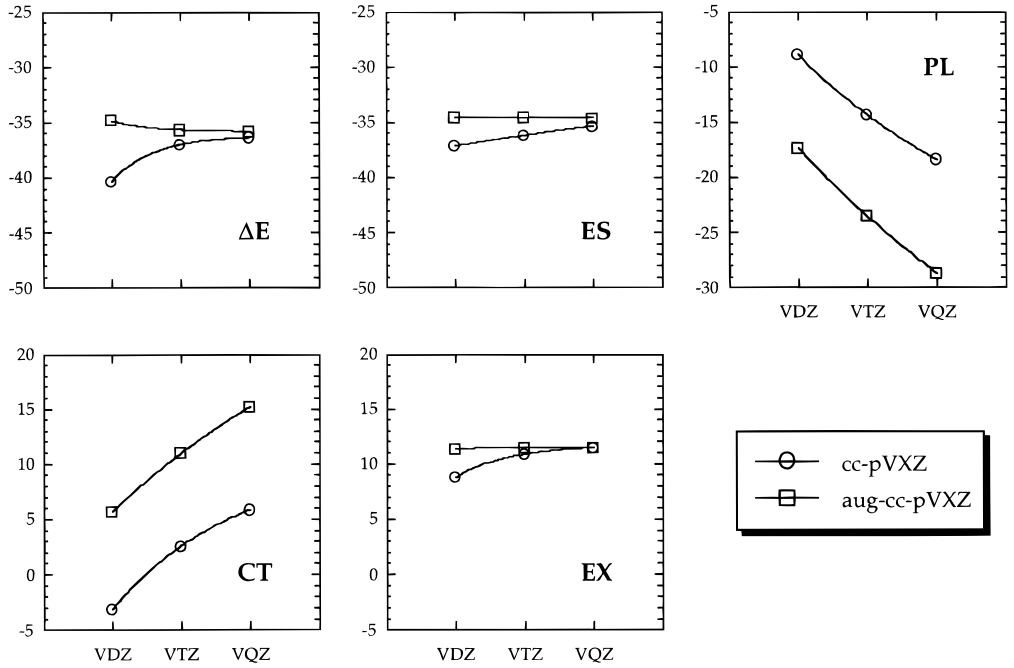

Figure 4. Convergence of the Morokuma components (in kcal mol^{-1}) for $Li^+(H_2O)$ as a function of basis set level. The curves are obtained from exponential fits (eq 13) of the raw cc-pVXZ and aug-cc-pVXZ values.

NEDA calculates an induced dipole on water of 1.01 D. The small induced dipole at Li^+ (0.01 D) suggests only weak polarization of the cation by water, consistent with the negligible polarizability of Li^+. Exchange and charge transfer only weakly stabilize the complex. EX is almost negligible at −2.2 kcal mol^{-1}, only 6% of the binding energy. CT is somewhat larger (−6.2 kcal mol^{-1}, or 17% of ΔE) but remains weak, suggesting that the Li−O bond is predominantly ionic.

We have generally found that Pople's 6-31+G* basis set[35] provides a fairly reliable description of clusters consisting of an alkali metal cation with one to several oxygen-containing molecules.[9,11,12,15,16] This basis set is roughly of double-ζ quality and includes a set of polarization and diffuse functions on all heavy atoms. Previous work has shown that 6-31+G* performs remarkably well, often yielding CP-corrected binding energies that are in better agreement with the CBS limit than values calculated at either the cc-pVDZ or aug-cc-pVDZ level.[9,12] Figures 2 and 3 compare 6-31+G* NEDA results (the dashed lines) to those calculated with the correlation consistent basis sets. While 6-31+G* yields a binding energy of −35.7 kcal mol^{-1}, only 0.1 kcal mol^{-1} weaker than the apparent limit, cc-pVDZ and aug-cc-pVDZ give −37.3 and −34.7 kcal mol^{-1}, respectively, each differing from the CBS limit by more than 1.0 kcal mol^{-1}.

Comparison of the CBS and 6-31+G* components in Figure 2 reveals why the latter performs so well. While the CT, EX, and DEF(Li^+) components are in good agreement with the CBS limits, ES, POL, and, to a lesser extent, DEF(H_2O) are not. The ES and POL components clearly show the largest discrepancies. At the 6-31+G* level, ES is 4.3 kcal mol^{-1} too strong while POL is 5.8 kcal mol^{-1} too weak. That is, NEDA suggests that 6-31+G* overestimates the strength of the electrostatic interaction but underestimates the contribution from polarization. These errors are roughly offsetting so that the resulting binding energy is in nearly exact agreement with the CBS limit.

Additional evidence suggesting that the 6-31+G* basis set overestimates ES and underestimates POL is found in the static dipole and polarizability of water and in the induced dipole of water in the $Li^+(H_2O)$ complex. The 6-31+G* dipole moment of water at the experimental geometry is 2.33 D, about 20% larger than the estimated CBS limit of 1.98 D.[24] Thus, 6-31+G* should overestimate the strength of the electrostatic interaction with Li^+ (as revealed by NEDA). On the other hand, the 6-31+G* polarizability of water is 5.99 a_0^3, roughly 30% smaller than the estimated CBS limit of 8.54 a_0^3.[24] Hence, 6-31+G* should underestimate the degree of polarization of the water molecule. Furthermore, NEDA evaluates an induced dipole moment on water in $Li^+(H_2O)$ of 0.76 D at the 6-31+G* level, 25% smaller than the CBS limit of 1.01 D. In short, 6-31+G* yields a binding energy for $Li^+(H_2O)$ that is in good agreement with highly extended basis set calculations. This agreement is, however, fortuitous, relying on the cancellation of errors that stem from the inability of this basis set to accurately describe the moments and polarizability of the water molecule.

We now proceed with a 6-31+G* analysis of the $M^+(H_2O)_n$ complexes. Despite its deficiencies, this basis set level is capable of producing at least semiquantitative results that provide insight into the nature of cation−ligand interactions.

IV. $M^+(H_2O)$ Complexes

We first focus attention on cation−water interactions in complexes consisting of an alkali metal cation (Li^+, Na^+, K^+, Rb^+, and Cs^+) with a single water molecule. NEDA results for these complexes are listed in Table 1. Calculations were performed on structures of C_{2v} symmetry, the cation collinear with the bisector of the HOH bond angle. The M−O distances were fixed at near-equilibrium values (cf. footnote of Table 1) and the water molecule was constrained to the experimentally determined geometry [R(OH) = 0.9572 Å, ∠(HOH) = 104.52°].[23] The 6-31+G* basis set was employed for all atoms except K, Rb, and Cs. The latter were each treated with an effective core potential (ECP) and a (5s5p)/[3s2p] valence basis set augmented by a single 6-term, d-type polarization function.[36] The outer-

(35) Hehre, W. J.; Radom, L.; Schleyer, P. v. R.; Pople, J. A. *Ab Initio Molecular Orbital Theory*; Wiley: New York, 1986.

(36) Hay, P. J.; Wadt, W. R. *J. Chem. Phys.* **1985**, *82*, 299.

Table 1. Analysis of the $M^+(H_2O)$ Complexes[a]

M	ΔE	ES	POL	CT	EX	DEF(M^+)	DEF(H_2O)
Li	−35.7	−38.9	−19.1	−5.7	−2.2	12.1	18.1
Na	−25.2	−29.2	−15.3	−2.0	−2.5	9.5	14.4
K	−18.7	−21.7	−9.0	−1.6	−2.2	9.6	6.2
Rb	−16.0	−18.4	−7.8	−1.1	−2.0	8.3	5.0
Cs	−13.8	−16.1	−7.0	−1.1	−1.9	8.1	4.2

[a] 6-31+G* values. All energy values in kcal mol^{-1}. Geometrical parameters were constrained to the following values (C_{2v} symmetry): R(Li−O) = 1.85 Å, R(Na−O) = 2.23 Å, R(K−O) = 2.67 Å, R(Rb−O) = 2.90 Å, R(Cs−O) = 3.14 Å, R(OH) = 0.9572 Å, ∠(HOH) = 104.52°.

Table 2. Comparison of NEDA and Classical Induced Dipole Moments of the $M^+(H_2O)$ Complexes[a]

M	$\Delta\mu(M^+)$	eq 14	$\Delta\mu(H_2O)$	eq 15
Li	0.01	0.01	0.76	1.11
Na	0.02	0.02	0.62	0.77
K	0.17	0.14	0.40	0.54
Rb	0.20	0.19	0.36	0.46
Cs	0.25	0.26	0.32	0.40

[a] 6-31+G* values. Induced dipole moments in D. See footnote of Table 1 for geometrical parameters. R is the distance from the cation to the water center of mass. Other parameters for eqs 14 and 15: $q(M^+) = 1.0$, $\mu(H_2O) = 2.33$ D, $\alpha(H_2O) = 5.711$, $\alpha(Li^+) = 0.061$, $\alpha(Na^+) = 0.346$, $\alpha(K^+) = 4.063$, $\alpha(Rb^+) = 7.322$, $\alpha(Cs^+) = 12.209$ (polarizabilities in a_0^3).

most ($n - 1$) shell of core electrons (*e.g.*, 3s and 3p in K) was treated explicitly in the Hartree−Fock equations, the field of the remaining core electrons being described by the ECP. Additional details of the basis sets have been given elsewhere.[9] We have previously shown[11] that RHF calculations with this basis set yield binding enthalpies (298 K) for the $M^+(H_2O)$ complexes within 1.0 kcal mol^{-1} of the experimentally determined values.[37]

Electrostatic and polarization effects are primarily responsible for the interaction of the alkali cations with water. The binding energies for the $M^+(H_2O)$ complexes diminish as the size of the cation increases from Li^+ ($\Delta E = -35.7$ kcal mol^{-1}) to Cs^+ ($\Delta E = -13.8$ kcal mol^{-1}). The ES and POL components listed in Table 1 exhibit similar behavior and are the dominant attractive contributions to the interaction. ES is a few kcal mol^{-1} stronger than ΔE for each complex and POL is typically about 50% as strong as ES. The limited covalent character of the M−O bond is clearly revealed by the weak CT contributions that are less than 10% of ΔE for all cations except Li^+.

Induced dipole moments calculated by NEDA are in general accord with the values predicted from a classical treatment of polarizable charge distributions. Table 2 compares the NEDA dipoles for the cations and water molecules with those obtained from the approximations[33,34]

$$\Delta\mu(M^+) = \frac{2\alpha(M^+)\mu(H_2O)}{R^3} \tag{14}$$

$$\Delta\mu(H_2O) = \frac{q(M^+)\alpha(H_2O)}{R^2} \tag{15}$$

where q, μ, and α are respectively the static charge, dipole moment, and polarizability of the fragments (see the footnote of Table 2). The NEDA and classical dipoles for the cation are essentially identical, differing by only 0.03 D or less. The Cs^+ cation is highly polarizable ($\alpha = 12.209\ a_0^3$) so that the neighboring water molecule induces a fairly sizable dipole

(37) Dzidic, I.; Kebarle, P. *J. Phys. Chem.* **1970**, *74*, 1466.

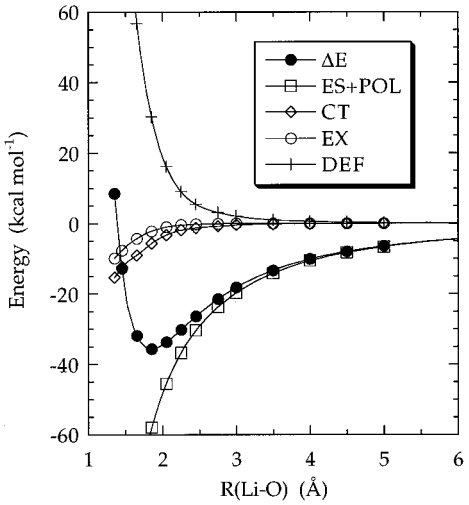

Figure 5. Variation in the binding energy and components for the $Li^+(H_2O)$ complex as a function of Li−O distance.

(∼0.25 D) at this site. In contrast, Li^+ cation is essentially unpolarizable ($\alpha = 0.061\ a_0^3$) so that it has effectively no induced moment (only 0.01 D).

The NEDA and classical moments for water differ somewhat, the NEDA values tending to be somewhat smaller than the classical values. For example, we calculated an induced dipole on the water molecule in $Li^+(H_2O)$ of 0.76 D, 0.35 D smaller than the value predicted by eq 15. It appears that the differing behavior of the NEDA and classical dipoles is a direct result of Pauli repulsions that are not considered in eqs 14 and 15. In a classical treatment, the water molecule can freely polarize in the field of the cation, regardless of the M−O bond length. By requiring that the wave functions $\psi^{\mathrm{def}}_{M^+}$ and $\psi^{\mathrm{def}}_{H_2O}$ remain orthogonal, the NEDA approach effectively prevents the water from freely polarizing toward the cation at short bond lengths. In essence, the water molecule becomes less polarizable for small cation−water separations and the induced dipole moment on water increases less rapidly than anticipated. The cation is, however, essentially free to polarize since its electron distribution shifts away from the water molecule.

A somewhat more detailed picture of electrostatic interaction and polarization can be obtained by examining the M−O bond length dependence of the NEDA quantities. Figure 5 shows a representative decomposition of the potential energy curve for $Li^+(H_2O)$. The long-range behavior of this potential is clearly dominated by electrostatic interaction and polarization effects; the ΔE and ES + POL curves overlap strongly for Li−O distances longer than 3.5 Å. Even at 3.0 Å, roughly van der Waals' contact, the ΔE and ES + POL values (−18.2 and −19.8 kcal mol^{-1}, respectively) differ by less than 2 kcal mol^{-1}. Similar behavior is found for the other $M^+(H_2O)$ complexes (data not shown).

The bond length dependence of ES and POL is similar to that expected from the classical treatment of the $M^+(H_2O)$ complexes. Figure 6 shows the ES components for the five complexes as a function of M−O distance. These values overlap fairly well with the classical result (the dashed curve) of a point charge interacting with the static water dipole moment (2.33 D at 6-31+G*, experimental geometry). Figure 7 compares the corresponding POL components to the classical treatment of polarizable water ($\alpha_{zz} = 5.711\ a_0^3$) interacting with a point charge. The POL values for $Li^+(H_2O)$ are in excellent agreement with the classical (dashed) curve. However, the POL values for the heavier cations, particularly Rb^+ and Cs^+, tend to be stronger than predicted. This difference arises, in part,

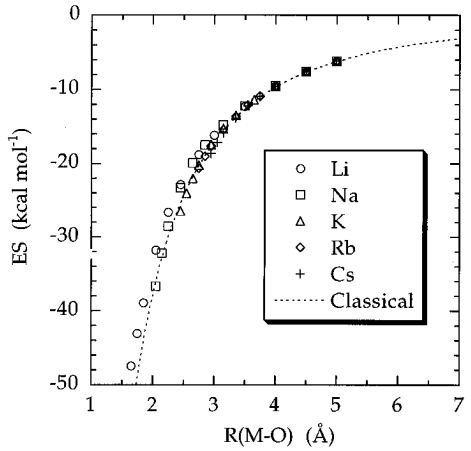

Figure 6. Comparison of the $M^+(H_2O)$ ES components with the classical charge-dipole approximation as a function of M−O distance.

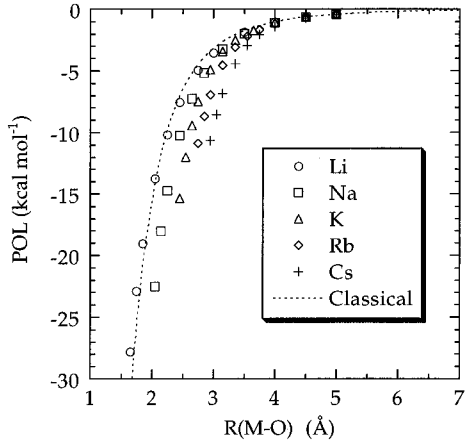

Figure 7. Comparison of the $M^+(H_2O)$ POL components with the classical charge-dipole polarizability approximation as a function of M−O distance.

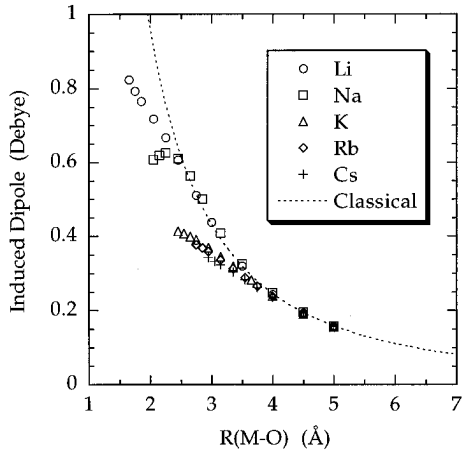

Figure 8. Comparison of the water induced dipole moment in the $M^+(H_2O)$ complexes with the classical charge-dipole polarizability approximation as a function of M−O distance.

from the additional polarization of the cation by the dipole moment of the water molecule, an effect that is negligible for the hard Li^+ cation.

The bond length dependence of the induced dipole on water is well represented by a classical electrostatic treatment, except at relatively short M−O bond lengths. Figure 8 compares the NEDA dipoles for the five cation−water complexes to the classical result (the dashed curve) based on the interaction of polarizable water with a point charge. In general, we find that

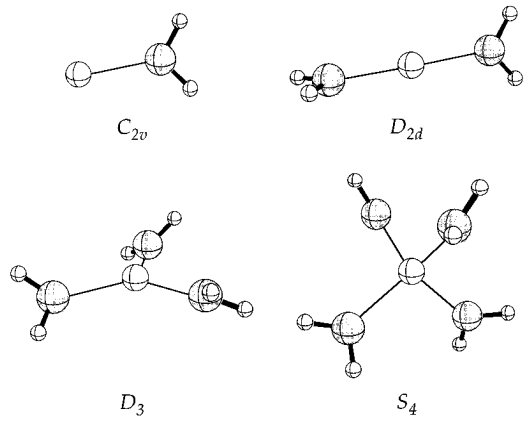

Figure 9. Geometries of the $M^+(H_2O)_n$ complexes.

Table 3. Optimized Geometries of the $M^+(H_2O)_n$ Complexes[a]

n	*R*(M−O)	*R*(OH)	∠(HOH)
	$Li^+(H_2O)_n$		
1	1.850	0.954	106.4
2	1.878	0.953	106.6
3	1.915	0.952	106.7
4	1.969	0.951[b]	106.8
	$Na^+(H_2O)_n$		
1	2.230	0.953	105.6
2	2.249	0.952	105.7
3	2.277	0.951	105.9
4	2.306	0.950[b]	106.1
	$K^+(H_2O)_n$		
1	2.669	0.952	105.4
2	2.706	0.951	105.5
3	2.730	0.951	105.6
4	2.759	0.950[b]	105.8
	$Rb^+(H_2O)_n$		
1	2.902	0.951	105.3
2	2.938	0.951	105.4
3	2.960	0.950	105.6
4	2.987	0.950[b]	105.7
	$Cs^+(H_2O)_n$		
1	3.136	0.951	105.3
2	3.178	0.950	105.4
3	3.201	0.950	105.6
4	3.228	0.950[b]	105.7

[a] 6-31+G* values. Bond lengths in Å and bond angles in deg. The complexes have C_{2v}, D_{2d}, D_3, and S_4 symmetry for $n = 1-4$, respectively. The optimized parameters for an isolated water molecule are $R(OH) = 0.948$ Å and $\angle(HOH) = 106.5°$. [b] Average length of the two symmetry unique bonds. The actual values differ by less than 0.001 Å.

the long-range behavior of the NEDA moment mimics that of the classical polarizable charge distribution. However, at shorter distances, typically within van der Waals' contact where the cation and water distributions overlap strongly, the NEDA moments deviate from the classical values. Again, this suggests that water is unable to freely polarize when it comes in contact with the cation.

V. $M^+(H_2O)_n$ Complexes ($n = 2-4$)

Larger aqueous clusters of the alkali cations were examined to determine the influence of multiple waters on the NEDA components and dipole moments. Calculations on the high symmetry structures shown in Figure 9 were performed at the same basis set level described in the previous section. Details of the optimized structures[11] are given in Table 3. In general, we find that the M−O distances increase slightly with increasing coordination [from 1.850 Å in $Li^+(H_2O)$ to 1.969 Å in $Li^+(H_2O)_4$] and that the geometry of a water molecule coordinating a cation is almost identical to that at infinite separation.

Table 4. Analysis of the $M^+(H_2O)_n$ Clusters[a]

n	$\Delta E/n$[b]	ES/n	POL/n	CT/n	EX/n	DEF(M^+)/n	DEF(H_2O)	$\Delta\mu(H_2O)$	$q(M^+)$[c]
					$Li^+(H_2O)_n$				
1	−35.6	−39.1	−18.8	−5.8	−2.2	12.0	18.1	0.75	0.993
2	−33.2	−36.3	−16.3	−12.7	−2.2	11.1	23.2	0.68	0.966
3	−29.9	−33.4	−14.1	−18.3	−2.3	9.7	28.4	0.61	0.931
4	−26.5	−30.2	−12.8	−21.6	−2.4	7.9	32.6	0.53	0.901
					$Na^+(H_2O)_n$				
1	−25.1	−29.3	−15.2	−2.1	−2.5	9.4	14.5	0.61	0.998
2	−23.7	−27.4	−13.4	−3.7	−2.3	8.8	14.3	0.58	0.990
3	−22.0	−25.8	−11.0	−5.3	−2.1	7.9	14.2	0.51	0.978
4	−20.2	−23.8	−9.7	−6.8	−2.0	7.1	15.0	0.46	0.964
					$K^+(H_2O)_n$				
1	−18.6	−21.7	−8.9	−1.6	−2.2	9.6	6.3	0.39	0.999
2	−17.6	−20.5	−7.1	−2.0	−2.0	8.3	5.7	0.34	0.998
3	−16.6	−19.5	−6.0	−2.6	−1.8	7.6	5.6	0.29	0.994
4	−15.6	−18.2	−5.1	−3.1	−1.6	6.9	5.6	0.24	0.989
					$Rb^+(H_2O)_n$				
1	−15.8	−18.3	−7.6	−1.1	−2.0	8.2	5.0	0.36	1.000
2	−15.0	−17.4	−6.3	−1.3	−1.8	7.2	4.5	0.32	0.999
3	−14.3	−16.6	−5.5	−1.6	−1.7	6.7	4.4	0.28	0.997
4	−13.5	−15.7	−4.7	−2.0	−1.5	6.1	4.4	0.24	0.994
					$Cs^+(H_2O))_n$				
1	−13.7	−16.1	−7.0	−1.1	−1.9	8.1	4.2	0.32	1.001
2	−12.9	−15.2	−5.7	−1.1	−1.7	7.0	3.7	0.28	1.000
3	−12.4	−14.6	−5.1	−1.3	−1.6	6.6	3.6	0.25	0.999
4	−11.7	−13.8	−4.4	−1.6	−1.5	6.0	3.5	0.22	0.998

[a] 6-31+G* values for geometries listed in Table 3. All energy values in kcal mol^{-1} and induced dipole moments in D. The DIS(H_2O) contributions (<0.1 kcal mol^{-1}) are not listed. [b] Energy change for the reactions $M^+ + nH_2O \rightarrow M^+(H_2O)_n$. [c] Atomic charge of the metal center.

The binding energies and components for the $M^+(H_2O)_n$ clusters are listed in Table 4. Average quantities (energy per water molecule) are reported for the reactions

$$M^+ + nH_2O \rightarrow M^+(H_2O)_n$$

where the reactant waters are at the RHF/6-31+G* optimized geometry. Distortion contributions to the binding energy (DIS of eq 11) arising from the change in fragment geometry during association are less than 0.1 kcal mol^{-1} per water molecule and are not listed. Table 4 also reports the induced dipoles on the water molecules and the charge on the metal center (evaluated by natural population analysis).[7,18]

The average binding energy of water diminishes with increasing coordination of the M^+ cation. NEDA suggests that ES and POL are primarily responsible for this trend. For instance, the electrostatic interaction per water molecule in $Li^+(H_2O)_4$ is nearly 9 kcal mol^{-1} weaker than that of $Li^+(H_2O)$ (−30.2 vs −39.1 kcal mol^{-1}), the direct result of unfavorable dipole−dipole interactions in the larger cluster. Polarization effects also weaken (from −18.8 to −12.8 kcal mol^{-1}) due to the unfavorable interactions of the ligands. This effect is revealed in the induced dipoles at water that decrease from 0.75 D in $Li^+(H_2O)$ to 0.53 D in $Li^+(H_2O)_4$.

Steric repulsions also act to destabilize the larger $Li^+(H_2O)_n$ clusters and reduce the binding energies. The effect is clearly revealed in the repulsive DEF(H_2O) contributions that strengthen with increasing coordination. This trend arises from increasing ligand overlap (Pauli repulsions) with successive additions of water to the $Li^+(H_2O)_n$ clusters. Similar behavior was recently reported for clusters of Li^+ with dimethyl ether.[12] For the K^+, Rb^+, and Cs^+ clusters, we calculate the opposite trend, the DEF(H_2O) contributions diminishing with increasing coordination. This suggests the heavy cations are sufficiently large that steric repulsion remains weak. The $Na^+(H_2O)_n$ clusters are an intermediate case for which DEF(H_2O) remains fairly constant for all cluster sizes.

Charge transfer in the $M^+(H_2O)_n$ clusters strengthens with increasing cluster size, a trend that seems counterintuitive. CT arises primarily from the delocalization of electrons from an oxygen lone pair (donor) into the valence s orbital (acceptor) of the metal. One would generally anticipate that CT interactions would weaken as additional electron donors interact with a single acceptor. The first interaction transfers a small amount of electron density to the cation, presumably rendering the cation a weaker acceptor for additional interactions. However, natural population analysis and NEDA reveal the opposite trend. For instance, based on the charge of Na^+ in the $Na^+(H_2O)_n$ clusters (last column of Table 4), we judge that the first water only transfers 0.002 electrons to the metal cation whereas the second through fourth transfer 0.008, 0.012, and 0.014 electrons, respectively. Thus, it appears that the M−O bond gains covalent character with increasing coordination. Similar CT effects were reported for Li^+−dimethyl ether clusters.[12]

VI. UHF Applications: $Na(H_2O)_n$ Clusters ($n = 1-4$)

We demonstrate the UHF NEDA approach by examining the interactions of water with Na atom in the $Na(H_2O)_n$ clusters. The structure of these clusters and the location of the unpaired valence electron of Na are issues of current debate.[38−44] Barnett and Landman[39] analyzed the charge distribution for cluster sizes up to $Na(H_2O)_8$ using density functional theory (DFT). The largest of these clusters had Na embedded in either a tetrahedral or octahedral shell of water molecules. Their analysis suggested

(38) Hertel, I. V.; Huglin, C.; Nitsch, C.; Schulz, C. P. *Phys. Rev. Lett.* **1991**, *67*, 1767.
(39) Barnett, R. N.; Landman, U. *Phys. Rev. Lett.* **1993**, *70*, 1775.
(40) Hashimoto, K.; He, S.; Morokuma, K. *Chem. Phys. Lett.* **1993**, *206*, 297.
(41) Hashimoto, K.; Morokuma, K. *Chem. Phys. Lett.* **1994**, *223*, 423.
(42) Hashimoto, K.; Morokuma, K. *J. Am. Chem. Soc.* **1994**, *116*, 11436.
(43) Dhar, S.; Kestner, N. R. *Radiat. Phys. Chem.* **1988**, *32*, 355.
(44) Kestner, N. R.; Dhar, S. *Large Finite Systems*; Jortner, J., Pullman, A., Pullman, B., Eds.; Reidel Publishing: Boston, 1987; pp 209−215.

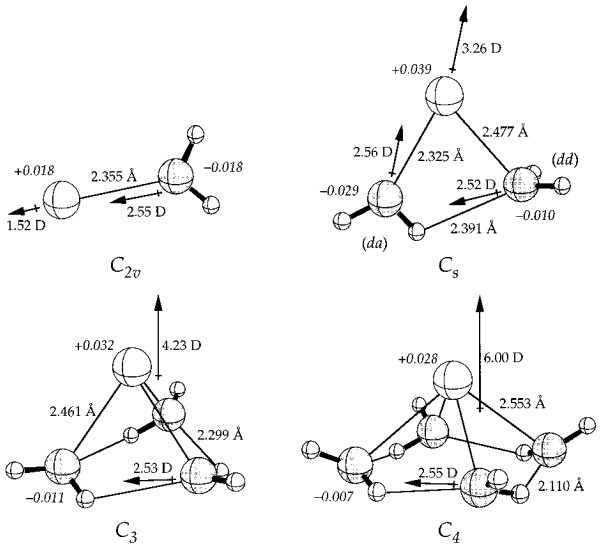

Figure 10. 6-31+G* optimized geometries for the $Na(H_2O)_n$ ($n = 1$, 2) complexes. Fragment dipole moments were evaluated by the NEDA approach. Charges on the fragments are given in italics.

that hydration in the larger clusters facilitates the delocalization of the unpaired electron over the solvation shell, thereby forming Na^+. Similar conclusions were reported by Dhar and Kestner.[43,44] The *ab initio* calculations of Hashimoto and Morokuma[40−42] revealed, however, cluster geometries of lower energy than those examined in the DFT study. Several lower energy geometries were identified, each resembling a Na atom resting on the surface of a $(H_2O)_n$ cluster and directly interacting with only three or four water molecules. The unpaired electron remained localized on Na in these alternative structures.

Calculations of the $Na(H_2O)_n$ clusters ($n = 1-4$) were performed at the UHF/6-31+G* level. The optimized geometries shown in Figure 10 are identical to those reported by Hashimoto and Morokuma[40−42] at the same level of theory. The $Na(H_2O)$ structure resembles the cation complex $Na^+(H_2O)$ with the water dipole directed toward the metal in a C_{2v} configuration. The most significant difference between the neutral and cation complex is the Na−O distance which is 0.125 Å longer in $Na(H_2O)$ than $Na^+(H_2O)$ (2.355 vs 2.230 Å). The $Na(H_2O)_2$ cluster has C_s symmetry and resembles a Na atom interacting with the water dimer. The $Na(H_2O)_3$ and $Na(H_2O)_4$ clusters respectively resemble a Na atom interacting with a cyclic water trimer and tetramer. Natural population analysis reveals that the unpaired electron remains localized on Na in these clusters, consistent with the conclusions of Hashimoto and Morokuma.[40−42] The charge on Na (shown in italics in Figure 10) ranges from +0.02 to −0.04, reflecting only weak delocalization of the unpaired electron onto the water molecules.

CP-corrected binding energies and components were evaluated at the UHF/6-31+G* level for the reactions

$$Na + nH_2O \rightarrow Na(H_2O)_n$$

where the reactant water molecules are at the RHF/6-31+G* optimized geometry. Average values (energy per water molecule) are reported in Table 5. Note that the average binding energy strengthens with increasing n due to the hydrogen bonds formed between water molecules in the larger clusters. The opposite trend was calculated for the $M^+(H_2O)_n$ complexes. Our CP-corrected binding energies are 1−1.5 kcal mol^{-1} (∼20%) weaker than the uncorrected values reported by Hashimoto and Morokuma[42] at the same level of theory. Electron correlation effects are significant. The CP-corrected binding energies at

Table 5. Analysis of the $Na(H_2O)_n$ Clusters[a]

n	$\Delta E/n$[b]	ES/n	POL/n	CT/n	EX/n	DEF(Na)/n	DEF(H_2O)
1	−4.8	−24.6	−13.6	−13.3	−6.1	38.5	14.3
2	−5.3	−24.0	−11.6	−13.4	−5.7	31.3	18.2[c]
3	−5.8	−24.5	−10.4	−13.8	−5.7	24.6	23.9
4	−6.1	−23.7	−8.4	−14.8	−4.8	17.9	27.6

[a] 6-31+G* values. All values in kcal mol^{-1}. The DIS(H_2O) contributions (<0.1 kcal mol^{-1}) are not listed. [b] Energy change for the reactions $Na + nH_2O \rightarrow Na(H_2O)_n$. [c] Average of the DEF(*da*) and DEF(*dd*) values, 18.9 and 17.4 kcal mol^{-1}, respectively. The labels *da* and *dd* refer to the electron donor−acceptor and double-donor water molecules shown in Figure 10.

the MP2/6-31+G* level are typically 0.5−1 kcal mol^{-1} (∼10−15%) stronger than the corresponding UHF values. Hence, a correlated treatment of the $Na(H_2O)_n$ clusters is required to obtain a quantitative description of Na−water interactions. NEDA, however, cannot be applied in its present form to correlated methods. Nevertheless, we anticipate that the UHF treatment will reflect the essential characteristics of these clusters.

Electrostatic interaction is, perhaps surprisingly, the dominant attractive contribution to the binding energies of the $Na(H_2O)_n$ complexes. NEDA calculates an ES component for $Na(H_2O)$ of −24.6 kcal mol^{-1}, nearly as strong as that of $Na^+(H_2O)$, −29.3 kcal mol^{-1} (cf. Table 4). One might anticipate that electrostatic effects are negligible for the interaction of a polar molecule with a spherical, uncharged atom. This expectation is based, however, on a classical treatment of non-overlapping charge distributions, which is clearly not the case for $Na(H_2O)$. The water molecule significantly penetrates the Na atom, as suggested by the large DEF terms in Table 5. Penetration effects and the strong ES component weaken rapidly as the Na−O distance is increased. If the distance in lengthened to 4.0 Å, the ES contribution diminishes by 94%, from −24.6 to only −1.4 kcal mol^{-1}. In contrast, a similar lengthening of the Na−O distance in $Na^+(H_2O)$ reduces its ES component by only 67%. Thus, the strong electrostatic interaction in the $Na(H_2O)$ complex is short range, arising from the penetration of the water and Na atom charge distributions.

Polarization effects are clearly visible in the $Na(H_2O)_n$ clusters. Strong dipoles are induced on the Na and water fragments, as shown in Figure 10. Successive addition of water to the clusters strengthens the dipole at Na by about 1.5 D per water, from 1.53 D in $Na(H_2O)$ to 6.00 D in $Na(H_2O)_4$. Each water molecule has a dipole of roughly 2.5 D compared to 2.29 D at infinite separation (6-31+G* optimized geometry). In general, we find that the water molecules polarize toward an adjacent hydrogen bonded water while Na polarizes away from the water cluster.

VII. Summary

Natural energy decomposition analysis (NEDA) provides an efficient and numerically stable quantum-mechanical approach for quantitatively assessing the contributions to molecular interaction potentials. In this paper, we have proposed a modification of the original method[5] that partitions the ES component into separate electrostatic, polarization, and exchange contributions. Thus, in its modified form, NEDA evaluates electrostatic (ES), polarization (POL), charge transfer (CT), exchange (EX), and deformation (DEF) components. NEDA further calculates the dipole moments induced on the fragments of a molecular cluster, thereby providing a quantitative measure of the degree of polarization experienced by each fragment in the field of its neighbors. The method is implemented at both

the restricted- and unrestricted-Hartree−Fock levels of theory in the GAMESS[20] version of the natural bond orbital (NBO) program.[18]

The NEDA applications presented here demonstrate the stability and reasonable behavior of the components and dipole moments. Although evaluated quantum mechanically, ES, POL, and the water dipole moments generally exhibit behavior predicted by a classical treatment of polarizable charge distributions. In the $M^+(H_2O)_n$ clusters, the average ES and POL contributions to the binding energy decrease with increasing coordination of the metal cation due to the unfavorable dipole−dipole interactions between water molecules. The dipole moments calculated by NEDA behave classically except for short-range interactions where Pauli repulsions prevent the fragment charge distributions from freely polarizing.

Acknowledgment. This research was supported by the Division of Chemical Sciences, Office of Basic Energy Sciences, U.S. Department of Energy under Contract No. DE-AC06-76RLO 1830. The author also acknowledges the support of Associated Western Universities, Inc. in the form of a postdoctoral fellowship under Grant No. DE-FG06-89ER-75522 with the U.S. Department of Energy. A portion of this work was completed with the computing resources at the National Energy Research Supercomputer Center, Livermore, CA. Pacific Northwest Laboratory is a multiprogram national laboratory operated by Battelle Memorial Institute.

Supporting Information Available: Tables containing raw data from the NEDA and Morokuma analysis of $Li^+(H_2O)$ for a variety of basis sets, both correlation consistent and Pople-style (2 pages). This material is contained in many libraries on microfiche, immediately follows this article in the microfilm version of the journal, can be ordered from the ACS, and can be downloaded from the Internet; see any current masthead page for ordering information and Internet access instructions.

JA951834Y